

Experimental study of the A dependence of inclusive hadron fragmentation

D. S. Barton,* G. W. Brandenburg,[†] W. Busza, T. Dobrowolski, J. I. Friedman,
 C. Halliwell,[‡] H. W. Kendall, T. Lyons, B. Nelson, L. Rosenson, and R. Verdier
Massachusetts Institute of Technology, Cambridge, Massachusetts 02139

M. T. Chiaradia, C. DeMarzo, C. Favuzzi, G. Germinario, L. Guerriero, P. LaVopa, G. Maggi,
 F. Posa, G. Selvaggi, P. Spinelli, and F. Waldner
Istituto di Fisica and Istituto Nazionale di Fisica Nucleare, Bari, Italy

D. Cutts, R. S. Dulude,[§] B. W. Hughlock, R. E. Lanou, Jr., and J. T. Massimo
Brown University, Providence, Rhode Island 02912

A. E. Brenner, D. C. Carey, J. E. Elias, P. H. Garbincius, and V. A. Polychronakos**
Fermi National Accelerator Laboratory, Batavia, Illinois 60510

J. Nassalski and T. Siemarczuk
Institute of Nuclear Research, Warsaw, Poland
 (Received 13 September 1982)

Data are presented on the inclusive production of π^\pm , K^\pm , p , and \bar{p} for π^+ , K^+ , and protons incident on nuclear targets at 100 GeV. The results cover the kinematic range $30 \leq P \leq 88$ GeV/c for $P_t = 0.3$ and 0.5 GeV/c. The observed A dependence of the invariant cross sections exhibits remarkable simplicity, which does not naturally follow from current models of particle production. The results show that the hypothesis of limiting fragmentation can be extended to include collisions with nuclei.

I. INTRODUCTION

The mechanism of hadron fragmentation and resultant particle production in high-energy hardron-hardron collisions is not well understood. In order to investigate the main features of the fragmentation process we have carried out an extensive experimental survey of the forward-particle spectra for incident pions, kaons, and protons, and a broad range of targets and incident energies. The results on the projectile and energy dependence of the spectra for a proton target have been presented previously.¹ In this paper we concentrate on the target dependence of the spectra.

There are several motivations for investigating projectile fragmentation from such apparently complex targets as nuclei. From the point of view of the study of the hypothesis of limiting fragmentation,² nuclear targets add a new dimension. Consider, for example, a hadron-nucleus collision in the rest frame of the incident hadron, i.e., in which the nucleus is the projectile. Two interesting questions arise.

(1) At high energies, do hadron targets fragment in an energy-independent way for projectiles consid-

erably more massive and complex than nucleons?

(2) If so, to what extent does the fragmentation depend on the projectile?

We know from previous hadron-nucleus experiments that at high energies the multiplication of hadrons within a nucleus is relatively weak.³ This has been interpreted as evidence of long formation times of the produced particles.⁴ If this is a correct interpretation, nuclear targets can be looked upon as filters analyzing the wave function of the projectile.⁵ From this point of view, the leading-particle spectra reflect that part of the wave function which has not been absorbed by the target.

Finally, the A dependence of the leading-particle spectra can give information on the rate of energy loss of strongly interacting particles as they pass through nuclear matter.⁶ In contrast to the extensive knowledge of the energy loss by ionization when charged particles pass through ordinary matter, little is known about the nuclear stopping power for hadrons. This information is not only important for a better understanding of the interactions that take place when two hadrons pass through each other, but also is needed for predicting the kind of nuclear densities that may be achieved in head-on collisions

TABLE I. Targets used in this experiment. Most data were taken with the thicker targets. The thin targets were used primarily for finite thickness corrections.

Target	A	Thickness (g cm^{-2})
C	12.0	1.37
		3.93
		5.79
Al	27.0	5.99
Cu	63.5	2.89
		5.94
		9.94
Ag	107.9	6.71
Pb	207.2	2.06
		4.00
		7.38

of large nuclei.⁶

Previous measurements of the A dependence of inclusive processes in the beam fragmentation region include π^\pm , K^\pm , p , and \bar{p} production in proton interactions at 24 GeV (Ref. 7), $\bar{\Lambda}^0$, Λ^0 , and K_s^0 production by protons at 300 GeV (Ref. 8), Ξ^0 production by protons at 400 GeV (Ref. 9), and neutron production by protons at 400 GeV (Ref. 10). In this experiment, we have measured the inclusive production of π^\pm , K^\pm , p , and \bar{p} in 100-GeV π^+ , K^+ and p collisions with C, Al, Cu, Ag, and Pb targets. Since essentially the same equipment was used in an earlier measurement of these same processes for a hydrogen target, an accurate comparison between hA and hp interactions, free of many systematic errors, is possible. Preliminary results of this experiment have been discussed in Ref. 11.

II. THE EXPERIMENTAL METHOD AND MEASURED CROSS SECTIONS

The data were collected using the Fermilab Single Arm Spectrometer facility in the M6E beam line. An incident positive beam of 100 GeV/c was used. The production of the fast secondaries was measured over a momentum range of $30 \leq P \leq 88$ GeV/c and transverse-momentum range $0.18 \leq P_t \leq 0.5$ GeV/c. Data were taken simultaneously for the nine reaction types ($\pi\pi$, πK , πp , etc.). Good π - K - p separation was achieved over the entire kinematic using the seven Čerenkov counters of the facility. Full details of the apparatus, data-taking, and analysis procedures are described in Ref. 1.

A list of the targets used in the experiment is given in Table I. Typical data consisted of a sequential set of measurements using the thickest targets of C, Al, Cu, Ag, and Pb along with an empty-target run at a fixed spectrometer momentum and angle

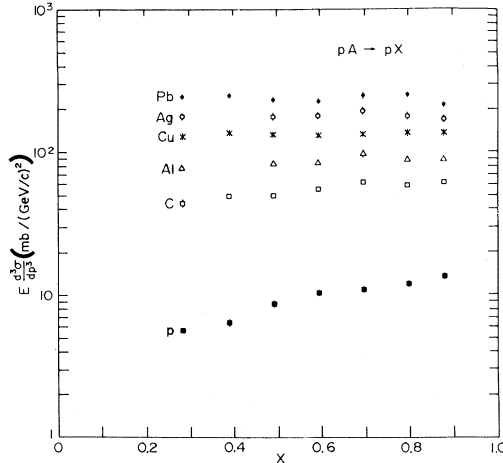


FIG. 1. The invariant differential cross section for $pA \rightarrow pX$ plotted as a function of x for an incident momentum of 100 GeV/c at transverse momentum of 0.3 GeV/c.

setting. In this way, the A dependence of the invariant cross sections for each channel could be studied without requiring detailed knowledge of absolute acceptance apertures, particle identification efficiencies, etc. The thinner targets were used at $P=40$ and 80 GeV/c to study finite-target-thickness effects by extrapolation to zero target thickness. The average corrections to the thick-target data were x independent and $\lesssim 8\%$.

In a manner similar to that described in Ref. 1, the interaction rates were corrected for particle absorption and decay in the spectrometer, multiple-scattering losses in the spectrometer, particle misidentification, and track-reconstruction ineffi-

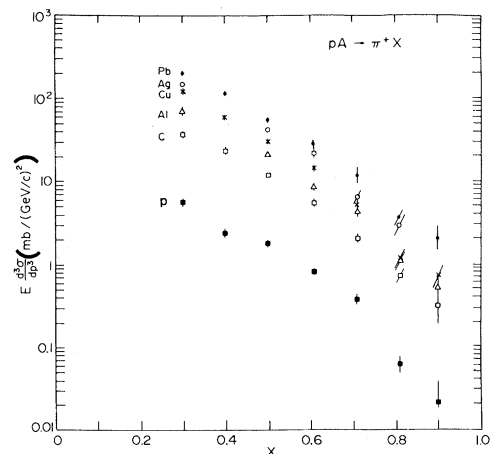


FIG. 2. The invariant differential cross section for $pA \rightarrow \pi^+X$ plotted as a function of x for an incident momentum of 100 GeV/c and transverse momentum of 0.3 GeV/c.

TABLE II. The measured inclusive invariant differential cross sections $E d^3\sigma/dp^3$ [in mb/(GeV/c)²], and the results of the fit of the data to the equation $E d^3\sigma/dp^3(A, x, P_t) = \sigma_0(x, P_t) A^{\alpha(x, P_t)}$. The errors shown for the measurements are primarily statistical, but contain a small contribution from particle misidentification (see text). In addition, there is an overall normalization uncertainty estimated to be 10%.

P_t	0.18 GeV/c				0.3 GeV/c				0.5 GeV/c					
	Reaction	p (GeV/c)	50	80	30	40	50	60	70	80	88	30	50	80
$\pi^+ p \rightarrow \pi^+ X$			6.43 ±0.22	5.20 ±0.20	4.55 ±0.18	4.385 ±0.088	4.335 ±0.094	4.390 ±0.070	4.99 ±0.11		3.61 ±0.15	1.930 ±0.059	1.619 ±0.028	
$\pi^+ C \rightarrow \pi^+ X$			54.1 ±2.2	41.08 ±0.84	37.0 ±1.0	32.1 ±1.2	30.01 ±0.71	28.17 ±0.61	29.76 ±0.46		30.1 ±1.4	15.72 ±0.83	11.11 ±0.42	
$\pi^+ Al \rightarrow \pi^+ X$			102.4 ±3.1		62.7 ±1.9	56.4 ±2.1	52.6 ±2.3	43.2 ±1.8	48.34 ±0.86					
$\pi^+ Cu \rightarrow \pi^+ X$			171.4 ±4.7	127.2 ±3.5	101.8 ±3.0	91.7 ±3.3	86.7 ±2.3	75.8 ±1.8	75.7 ±1.5		99.5 ±4.4	46.4 ±2.9	25.9 ±1.1	
$\pi^+ Ag \rightarrow \pi^+ X$			249.0 ±7.7		149.5 ±4.8	133.1 ±5.2	122.3 ±6.8	110.1 ±3.5	93.9 ±2.4					
$\pi^+ Pb \rightarrow \pi^+ X$			350 ±12	265.9 ±8.1	184.9 ±6.7	172.3 ±6.8	172 ±10	137.9 ±4.0	119.0 ±3.5		191.9 ±9.1	91.6 ±6.5	47.2 ±2.6	
σ_0 (mb)			11.56 ±0.74	8.01 ±0.37	8.94 ±0.47	7.62 ±0.52	6.38 ±0.36	6.78 ±0.30	8.74 ±0.29		6.07 ±0.56	3.37 ±0.39	3.14 ±0.27	
α			0.648 ±0.015	0.660 ±0.012	0.583 ±0.013	0.596 ±0.017	0.627 ±0.016	0.576 ±0.011	0.506 ±0.009		0.655 ±0.022	0.624 ±0.030	0.508 ±0.022	
$\pi^+ p \rightarrow \pi^- X$			2.00 ±0.15	1.295 ±0.070	3.56 ±0.14	2.039 ±0.075	1.120 ±0.041	0.978 ±0.036	0.836 ±0.032	0.659 ±0.032	0.469 ±0.023	1.78 ±0.11	0.682 ±0.038	0.141 ±0.018
$\pi^+ C \rightarrow \pi^- X$			16.04 ±0.92	10.93 ±0.64	28.1 ±1.4	17.70 ±0.71	8.07 ±0.52	6.94 ±0.35	6.29 ±0.32	5.24 ±0.33	4.03 ±0.24	16.41 ±0.86	4.76 ±0.37	1.08 ±0.13
$\pi^+ Al \rightarrow \pi^- X$					52.8 ±2.7		12.94 ±0.87	14.33 ±0.80	8.51 ±0.58	8.99 ±0.59	5.99 ±0.37			

TABLE II. (Continued.)

P_t	p (GeV/c)	0.18 GeV/c				0.3 GeV/c				0.5 GeV/c			
		50	80	30	40	50	60	70	80	88	30	50	80
$\pi^+ \text{Cu} \rightarrow \pi^- X$		46.1 ±2.6	32.9 ±1.7	99.1 ±4.9	52.9 ±1.8	21.1 ±1.4	23.0 ±1.2	21.3 ±1.1	15.32 ±0.89	11.18 ±0.69	48.5 ±2.7	15.0 ±1.1	3.09 ±0.35
$\pi^+ \text{Ag} \rightarrow \pi^- X$				130.7 ±9.7			30.4 ±1.8	27.7 ±2.0	24.3 ±1.7	14.5 ±1.1			
$\pi^+ \text{Pb} \rightarrow \pi^- X$		100.1 ±7.0	62.9 ±4.2	209 ±10	106.4 ±6.6	44.2 ±3.7	48.8 ±2.7	40.4 ±2.5	30.9 ±2.6	16.4 ±1.6	98.6 ±5.6	29.0 ±2.6	5.0 ±1.1
σ_0 (mb)		3.24 ±0.40	2.39 ±0.29	5.10 ±0.46	3.66 ±0.33	1.83 ±0.24	1.40 ±0.13	1.06 ±0.11	1.07 ±0.13	1.06 ±0.13	3.44 ±0.38	0.99 ±0.16	0.271 ±0.072
α		0.641 ±0.031	0.620 ±0.030	0.700 ±0.022	0.639 ±0.023	0.593 ±0.035	0.668 ±0.023	0.692 ±0.026	0.645 ±0.031	0.540 ±0.031	0.632 ±0.027	0.641 ±0.039	0.568 ±0.071
$\pi^+ p \rightarrow K^+ X$				0.66 ±0.12	0.493 ±0.081	0.380 ±0.069	0.237 ±0.030	0.222 ±0.027	0.190 ±0.017	0.196 ±0.023	0.350 ±0.077	0.205 ±0.026	0.070 ±0.008
$\pi^+ \text{C} \rightarrow K^+ X$				5.20 ±0.87	3.62 ±0.30	2.79 ±0.31	2.05 ±0.30	1.81 ±0.18	1.45 ±0.14	0.987 ±0.087	3.22 ±0.56	1.61 ±0.30	0.85 ±0.11
$\pi^+ \text{Al} \rightarrow K^+ X$				8.8 ±1.2		5.47 ±0.63	2.88 ±0.51	3.45 ±0.64	2.97 ±0.51	1.97 ±0.18			
$\pi^+ \text{Cu} \rightarrow K^+ X$				18.2 ±2.0	12.3 ±1.2	7.85 ±0.94	6.63 ±0.90	5.05 ±0.61	5.96 ±0.49	3.24 ±0.32	14.7 ±2.1	5.7 ±1.2	2.98 ±0.36
$\pi^+ \text{Ag} \rightarrow K^+ X$				17.0 ±3.0		12.0 ±1.6	9.0 ±1.4	6.9 ±1.8	4.50 ±0.86	6.08 ±0.63			
$\pi^+ \text{Pb} \rightarrow K^+ X$				28.0 ±4.9	23.1 ±3.0	18.5 ±2.4	11.8 ±2.0	8.0 ±2.6	8.1 ±1.0	7.68 ±0.88	22.8 ±4.2	13.1 ±2.9	3.92 ±0.85

TABLE II. (*Continued.*)

Reaction	P p (GeV/c)	0.18 GeV/c				0.3 GeV/c				0.5 GeV/c			
		50	80	30	40	50	60	70	80	88	30	50	80
σ_0 (mb)				1.31 ±0.36	0.71 ±0.13	0.58 ±0.12	0.38 ±0.11	0.44 ±0.11	0.354 ±0.067	0.163 ±0.028	0.62 ±0.20	0.26 ±0.10	0.214 ±0.060
α				0.583 ±0.069	0.667 ±0.049	0.646 ±0.053	0.658 ±0.069	0.579 ±0.071	0.607 ±0.047	0.737 ±0.043	0.702 ±0.079	0.74 ±0.10	0.584 ±0.073
$\pi^+ p \rightarrow K^- X$		0.172 ±0.065	0.055 ±0.016	0.408 ±0.072	0.330 ±0.041	0.160 ±0.019	0.105 ±0.014	0.069 ±0.010	0.031 ±0.009	0.012 ±0.004	0.155 ±0.064	0.097 ±0.019	0.010 ±0.007
$\pi^+ C \rightarrow K^- X$		1.39 ±0.37	0.42 ±0.11	2.86 ±0.57	2.13 ±0.31	1.14 ±0.23	0.63 ±0.11	0.67 ±0.12	0.337 ±0.075	0.073 ±0.032	2.50 ±0.43	0.84 ±0.18	0.167 ±0.058
$\pi^+ Al \rightarrow K^- X$				7.0 ±1.2		1.79 ±0.40	1.27 ±0.29	0.61 ±0.17	0.39 ±0.11	0.274 ±0.074			
$\pi^+ Cu \rightarrow K^- X$		3.7 ±1.0	1.06 ±0.29	8.8 ±1.8	6.77 ±0.82	2.73 ±0.60	2.73 ±0.43	2.41 ±0.35	0.76 ±0.18	0.32 ±0.11	7.3 ±1.3	2.52 ±0.50	0.40 ±0.19
$\pi^+ Ag \rightarrow K^- X$				19.7 ±4.5			3.33 ±0.67	4.05 ±0.73	1.69 ±0.36	0.52 ±0.19			
$\pi^+ Pb \rightarrow K^- X$		11.0 ±3.5	1.66 ±0.81	21.2 ±4.2	11.4 ±3.0	7.4 ±1.9	5.5 ±1.0	3.99 ±0.79	2.89 ±0.57		14.6 ±3.0	4.9 ±1.2	1.76 ±0.57
σ_0 (mb)		0.23 ±0.14	0.120 ±0.073	0.56 ±0.19	0.46 ±0.15	0.23 ±0.10	0.101 ±0.033	0.080 ±0.029	0.030 ±0.014	0.012 ±0.010	0.54 ±0.19	0.182 ±0.081	0.019 ±0.016
α		0.70 ±0.15	0.51 ±0.16	0.694 ±0.085	0.627 ±0.085	0.63 ±0.12	0.758 ±0.078	0.764 ±0.086	0.84 ±0.12	0.81 ±0.21	0.623 ±0.091	0.62 ±0.11	0.81 ±0.20
$\pi^+ p \rightarrow pX$				0.661 ±0.076	0.450 ±0.060	0.329 ±0.055	0.172 ±0.018	0.110 ±0.015	0.045 ±0.007	0.030 ±0.010	0.436 ±0.055	0.195 ±0.019	0.056 ±0.005

TABLE II. (Continued.)

Reaction	P_t	0.18 GeV/c				0.3 GeV/c				0.5 GeV/c				
		p (GeV/c)	50	80	30	40	50	60	70	80	88	30	50	
$\pi^+ C \rightarrow pX$			6.54 ±0.76	4.34 ±0.27	3.00 ±0.27	1.54 ±0.23	0.83 ±0.11	0.386 ±0.078	0.827 ±0.074		3.71 ±0.51	2.07 ±0.28	0.234 ±0.060	
$\pi^+ Al \rightarrow pX$			12.6 ±1.1		3.80 ±0.47	1.87 ±0.37	1.75 ±0.38	0.11 ±0.23	0.95 ±0.12					
$\pi^+ Cu \rightarrow pX$			21.8 ±1.7	14.4 ±1.1	7.40 ±0.78	5.10 ±0.70	2.38 ±0.35	1.10 ±0.24	1.24 ±0.21		13.4 ±1.7	5.48 ±0.97	0.59 ±0.17	
$\pi^+ Ag \rightarrow pX$			37.9 ±3.1		9.8 ±1.2	5.74 ±0.99	2.51 ±0.90	1.61 ±0.57	0.88 ±0.46					
$\pi^+ Pb \rightarrow pX$			44.4 ±4.4	27.3 ±2.7	16.1 ±1.9	7.4 ±1.4	4.6 ±1.5	2.76 ±0.64	0.56 ±0.64		31.3 ±4.2	13.9 ±2.4	0.88 ±0.44	
σ_0 (mb)			1.26 ±0.23	0.86 ±0.12	0.63 ±0.12	0.319 ±0.094	0.200 ±0.063	0.051 ±0.024	0.61 ±0.18		0.58 ±0.16	0.39 ±0.12	0.070 ±0.042	
α			0.690 ±0.043	0.660 ±0.037	0.592 ±0.050	0.611 ±0.074	0.588 ±0.088	0.73 ±0.12	0.131 ±0.096		0.750 ±0.066	0.656 ±0.078	0.49 ±0.16	
$\pi^+ p \rightarrow \bar{p}X$		0.103 ±0.028	0.008 ±0.004	0.260 ±0.043	0.160 ±0.022	0.090 ±0.011	0.044 ±0.008	0.025 ±0.004	0.007 ±0.003		0.165 ±0.042	0.053 ±0.013	0.007 ±0.005	
$\pi^+ C \rightarrow \bar{p}X$		1.28 ±0.26	0.128 ±0.079	2.81 ±0.43	0.87 ±0.19	0.47 ±0.17	0.17 ±0.11	0.658 ±0.098	0.062 ±0.034	0.019 ±0.024		1.72 ±0.28	0.272 ±0.083	0.23 ±0.11
$\pi^+ Al \rightarrow \bar{p}X$					4.55 ±0.80		0.74 ±0.32	0.03 ±0.37	0.69 ±0.25	0.37 ±0.15	0.053 ±0.064			
$\pi^+ Cu \rightarrow \bar{p}X$		2.77 ±0.70	0.14 ±0.20	7.9 ±1.4	3.24 ±0.53	1.24 ±0.48	0.65 ±0.38	0.87 ±0.36	0.56 ±0.21	0.026 ±0.048		5.29 ±0.90	1.27 ±0.29	0.29 ±0.29

TABLE II. (*Continued.*)

P_t	p (GeV/c)	0.18 GeV/c				0.3 GeV/c				0.5 GeV/c			
		50	80	30	40	50	60	70	80	88	30	50	80
$\pi^+ \text{Ag} \rightarrow \bar{p}X$				12.0 ± 3.2		0.89 ± 0.83	1.71 ± 0.72	0.40 ± 0.23	0.20 ± 0.14				
$\pi^+ \text{Pb} \rightarrow \bar{p}X$	5.4 ± 2.2	1.02 ± 0.77	23.0 ± 3.4	10.0 ± 2.3	4.5 ± 2.2	1.4 ± 1.4	3.0 ± 1.0	1.00 ± 0.54	1.22 ± 0.26	14.5 ± 2.2	1.74 ± 0.62	0.7 ± 2.0	
σ_0 (mb)	0.38 ± 0.19	0.032 ± 0.058	0.42 ± 0.13	0.101 ± 0.048	0.072 ± 0.061	0.020 ± 0.032	0.224 ± 0.098	0.009 ± 0.008		0.259 ± 0.089	0.056 ± 0.032	0.14 ± 0.27	
α	0.49 ± 0.14	0.50 ± 0.50	0.732 ± 0.075	0.85 ± 0.12	0.72 ± 0.23	0.80 ± 0.38	0.41 ± 0.13	0.88 ± 0.21		0.746 ± 0.082	0.68 ± 0.14	0.18 ± 0.63	
$K^+ p \rightarrow \pi^+ X$			3.75 ± 0.61	2.94 ± 0.63	2.46 ± 0.53	1.35 ± 0.20	0.62 ± 0.19	0.27 ± 0.13		2.91 ± 0.57	0.77 ± 0.18	0.209 ± 0.057	
$K^+ \text{C} \rightarrow \pi^+ X$			45.5 ± 8.2	23.6 ± 2.5	11.1 ± 2.4	10.2 ± 3.1	4.6 ± 1.2	1.71 ± 0.96	1.26 ± 0.61	18.3 ± 4.4	8.5 ± 2.3	0.89 ± 0.65	
$K^+ \text{Al} \rightarrow \pi^+ X$			47.7 ± 7.9		21.2 ± 5.0	28.8 ± 6.8	10.1 ± 4.2	2.5 ± 3.5	3.3 ± 1.3				
$K^+ \text{Cu} \rightarrow \pi^+ X$			136 ± 17	64.0 ± 9.9	49.8 ± 9.1	48 ± 11	20.4 ± 5.0	7.7 ± 4.1	1.1 ± 1.7	81 ± 19	16.7 ± 7.7	0.7 ± 1.6	
$K^+ \text{Ag} \rightarrow \pi^+ X$			153 ± 23		68 ± 15	56 ± 13	47 ± 18	8.8 ± 7.5	6.5 ± 4.4				
$K^+ \text{Pb} \rightarrow \pi^+ X$			256 ± 37	208 ± 25	105 ± 23	95 ± 21	72 ± 25	8.3 ± 9.3	7.5 ± 6.9	88 ± 31	37 ± 20	1.9 ± 3.9	
σ_0 (mb)			6.0 ± 1.9	3.52 ± 0.85	1.56 ± 0.61	2.01 ± 0.92	0.40 ± 0.22	0.36 ± 0.41	0.43 ± 0.49	4.5 ± 2.2	2.5 ± 1.8	0.7 ± 1.9	

TABLE II. (Continued.)

P_t	p (GeV/c)	0.18 GeV/c				0.3 GeV/c				0.5 GeV/c			
		50	80	30	40	50	60	70	80	88	30	50	80
α				0.706 ±0.076	0.744 ±0.061	0.804 ±0.094	0.73 ±0.11	0.97 ±0.14	0.66 ±0.30	0.47 ±0.33	0.60 ±0.12	0.48 ±0.21	0.07 ±0.86
$K^+p \rightarrow \pi^-X$		2.13 ±0.55		2.86 ±0.48	1.12 ±0.21	0.67 ±0.16	0.58 ±0.11	0.27 ±0.08	0.16 ±0.06		0.97 ±0.50	0.32 ±0.12	0.19 ±0.13
$K^+C \rightarrow \pi^-X$		20.8 ±4.8	1.83 ±0.92	25.3 ±5.5	18.8 ±2.8	9.8 ±2.2	3.8 ±1.1	2.53 ±0.67	1.21 ±0.60	0.42 ±0.29	7.6 ±2.7	3.1 ±1.3	0.57 ±0.29
$K^+Al \rightarrow \pi^-X$				35.4 ±8.8		13.9 ±3.6	7.4 ±1.9	3.7 ±1.4	2.3 ±1.2	0.76 ±0.37			
$K^+Cu \rightarrow \pi^-X$		78 ±16	4.0 ±2.5	77 ±17	47.6 ±6.5	20.4 ±4.9	19.9 ±4.3	8.0 ±2.5	3.3 ±1.8	2.3 ±1.1	36.6 ±9.8	11.9 ±3.7	1.62 ±0.77
$K^+Ag \rightarrow \pi^-X$					191 ±49		22.5 ±5.4	10.8 ±4.2	2.6 ±3.2	1.58 ±0.94			
$K^+Pb \rightarrow \pi^-X$		103 ±30	6.7 ±7.1	183 ±41	44 ±21	37 ±11	39.9 ±8.9	13.3 ±5.4	5.4 ±4.9	0.8 ±1.7	99 ±28	36 ±11	2.3 ±2.0
σ_0 (mb)		5.2 ±2.4	0.58 ±0.73	3.5 ±1.5	6.8 ±2.4	3.1 ±1.4	0.52 ±0.24	0.53 ±0.30	0.39 ±0.41	0.16 ±0.17	0.82 ±0.55	0.34 ±0.28	0.16 ±0.17
α		0.59 ±0.11	0.46 ±0.35	0.75 ±0.10	0.432 ±0.097	0.46 ±0.12	0.82 ±0.11	0.62 ±0.14	0.49 ±0.29	0.47 ±0.30	0.90 ±0.15	0.87 ±0.18	0.53 ±0.29
$K^+p \rightarrow K^+X$				2.62 ±0.86	2.23 ±0.70	2.07 ±0.62	1.47 ±0.28	1.75 ±0.27	2.54 ±0.23	3.01 ±0.37	1.17 ±0.74	1.14 ±0.23	0.86 ±0.10
$K^+C \rightarrow K^+X$				19.6 ±6.1	16.5 ±2.7	14.1 ±2.7	10.9 ±4.3	16.3 ±2.3	14.1 ±1.8	12.5 ±1.3	11.2 ±4.7	6.7 ±2.8	10.6 ±1.9

TABLE II. (*Continued.*)

P_t	p (GeV/c)	0.18 GeV/c				0.3 GeV/c				0.5 GeV/c			
		50	80	30	40	50	60	70	80	88	30	50	80
$K^+Al \rightarrow K^+X$		56 ±10		29.6 ±5.5	26.3 ±8.5	36.2 ±8.0	19.6 ±5.5	23.2 ±2.4					
$K^+Cu \rightarrow K^+X$		117 ±18	53 ±12	63 ±10	66 ±15	70.9 ±9.2	43.3 ±5.9	45.7 ±4.9	49 ±18	33 ±12	30.2 ±5.7		
$K^+Ag \rightarrow K^+X$		137 ±27		88 ±15	35 ±19	111 ±27	69 ±12	71.8 ±8.4					
$K^+Pb \rightarrow K^+X$		168 ±37	97 ±28	201 ±28	82 ±32	119 ±36	93 ±14	90 ±12	47 ±42	28 ±29	43 ±10		
σ_0 (mb)		4.7 ±1.8	3.4 ±1.3	1.42 ±0.47	2.7 ±1.7	2.52 ±0.74	2.50 ±0.67	2.15 ±0.41	2.7 ±2.4	1.5 ±1.4	3.1 ±1.2		
α		0.711 ±0.090	0.64 ±0.10	0.912 ±0.077	0.65 ±0.15	0.778 ±0.078	0.685 ±0.065	0.723 ±0.049	0.61 ±0.24	0.63 ±0.24	0.515 ±0.096		
$K^+C \rightarrow K^-X$	2.3 ±1.6		6.6 ±3.7	2.1 ±1.4	1.6 ±1.6	0.22 ±0.42	0.26 ±0.33				1.1 ±1.6		
$K^+Al \rightarrow K^-X$			12.6 ±7.4		3.1 ±2.0		0.65 ±0.52						
$K^+Cu \rightarrow K^-X$	5.1 ±7.4		23 ±21	5.4 ±3.0	6.0 ±5.5		1.2 ±1.3						
$K^+Ag \rightarrow K^-X$							4.6 ±4.9	1.8 ±3.4					
$K^+Pb \rightarrow K^-X$	8 ±25		41 ±34	15 ±13	12.3 ±9.8	3.8 ±6.1		3.4 ±6.1		9 ±58	5 ±16		

TABLE II. (Continued.)

P_t	p (GeV/c)	0.18 GeV/c				0.3 GeV/c				0.5 GeV/c			
		50	80	30	40	50	60	70	80	88	30	50	80
σ_0 (mb)		0.7 ± 1.6		1.4 ± 1.6	0.38 ± 0.58	0.30 ± 0.46							
α		0.46 ± 0.76		0.65 ± 0.32	0.66 ± 0.39	0.70 ± 0.39							
$K^+ C \rightarrow pX$				4.5 ± 2.5	2.42 ± 0.86	1.70 ± 0.73	1.37 ± 0.99	0.68 ± 0.49	0.51 ± 0.30	5.48 ± 0.78	4.1 ± 2.6	1.6 ± 2.5	0.55 ± 0.42
$K^+ Al \rightarrow pX$				7.9 ± 3.6		3.7 ± 1.6	3.3 ± 2.4	5.6 ± 3.6		10.6 ± 1.7			
$K^+ Cu \rightarrow pX$				10.6 ± 5.2	10.4 ± 3.9	8.0 ± 3.0	5.5 ± 3.4	0.6 ± 1.5	2.62 ± 0.92	5.3 ± 1.9	5 ± 12		1.1 ± 2.0
$K^+ Ag \rightarrow pX$				36 ± 12		2.7 ± 3.1	3.9 ± 4.1		1.6 ± 4.6				
$K^+ Pb \rightarrow pX$				13 ± 15	20 ± 17	12.9 ± 6.6	2 ± 11		6.0 ± 2.7	9.9 ± 5.5	20 ± 26	8 ± 31	
σ_0 (mb)				1.2 ± 1.2	0.34 ± 0.29	0.47 ± 0.39	0.49 ± 0.70	0.5 ± 1.3	0.066 ± 0.069	4.1 ± 1.8		1.3 ± 2.6	
α				0.56 ± 0.25	0.80 ± 0.24	0.56 ± 0.22	0.49 ± 0.39	0.17 ± 0.98	0.86 ± 0.24	0.14 ± 0.14		0.43 ± 0.61	
$K^+ C \rightarrow \bar{p}X$		2.1 ± 1.2	0.00 ± 0.36	1.9 ± 1.9	1.91 ± 0.94	1.3 ± 1.2		0.37 ± 0.45	0.00 ± 0.30	0.00 ± 0.12	2.4 ± 3.2	1.3 ± 1.2	0.00 ± 0.23
$K^+ Al \rightarrow \bar{p}X$				11.3 ± 5.2		2.2 ± 1.4	0.93 ± 0.74	0.7 ± 1.2	0.00 ± 0.65	0.30 ± 0.39			

TABLE II. (*Continued.*)

P_t	p (GeV/c)	0.18 GeV/c				0.3 GeV/c				0.5 GeV/c			
		50	80	30	40	50	60	70	80	88	30	50	80
$K^+Cu \rightarrow \bar{p}X$		6.9 ±4.0	0.0 ±1.1	5.7 ±5.8	6.1 ±2.2	3.0 ±1.9	1.8 ±1.1	1.7 ±1.7	0.00 ±0.90	0.00 ±0.35	11.6 ±6.3	4.3 ±2.5	1.6 ±1.7
$K^+Ag \rightarrow \bar{p}X$				21 ±21			0.0 ±2.0			0.00 ±0.90			
$K^+Pb \rightarrow \bar{p}X$		5. ±17	0.0 ±4.8	21 ±20	13.3 ±8.1	8.6 ±6.4	7.0 ±5.4	0.0 ±3.7		3.0 ±3.4	15 ±20		0.0 ±3.1
σ_0 (mb)		0.55 ±0.82		0.41 ±0.63	0.35 ±0.37	0.25 ±0.42	0.19 ±0.61	0.15 ±0.40			0.6 ±1.2		
α		0.57 ±0.43		0.74 ±0.39	0.68 ±0.26	0.63 ±0.42	0.48 ±0.80	0.42 ±0.83			0.67 ±0.49		
$pp \rightarrow \pi^+X$				5.56 ±0.27	2.37 ±0.19	1.80 ±0.17	0.82 ±0.05	0.375 ±0.033	0.063 ±0.014	0.022 ±0.018	2.46 ±0.16	0.658 ±0.043	0.041 ±0.006
$pC \rightarrow \pi^+X$				36.7 ±2.2	23.21 ±0.78	11.91 ±0.69	5.51 ±0.58	2.08 ±0.22	0.74 ±0.13	0.332 ±0.068	18.4 ±1.4	5.56 ±0.63	0.175 ±0.075
$pAl \rightarrow \pi^+X$				69.6 ±3.2		20.9 ±1.4	8.6 ±1.0	4.31 ±0.70	1.09 ±0.39	0.54 ±0.12			
$pCu \rightarrow \pi^+X$				120.7 ±5.0	58.1 ±3.0	31.0 ±2.0	14.5 ±1.6	5.23 ±0.65	1.17 ±0.34	0.72 ±0.22	51.6 ±4.1	16.5 ±2.2	0.85 ±0.28
$pAg \rightarrow \pi^+X$				145.8 ±7.6		41.1 ±3.3	21.8 ±2.6	6.4 ±1.6	2.93 ±0.73	0.55 ±0.27			
$pPb \rightarrow \pi^+X$				196 ±12	113.3 ±7.0	54.7 ±4.9	28.3 ±3.8	11.8 ±2.9	3.69 ±0.82	2.10 ±0.61	108.3 ±9.6	20.8 ±4.7	1.53 ±0.68

TABLE II. (Continued.)

P_t	p (GeV/c)	0.18 GeV/c				0.3 GeV/c				0.5 GeV/c			
		50	80	30	40	50	60	70	80	88	30	50	80
σ_0 (mb)				9.65 ±0.92	5.83 ±0.47	3.24 ±0.38	1.25 ±0.26	0.54 ±0.13	0.175 ±0.071	0.108 ±0.051	3.94 ±0.63	1.62 ±0.42	0.028 ±0.023
α				0.583 ±0.023	0.555 ±0.023	0.540 ±0.031	0.594 ±0.052	0.557 ±0.070	0.55 ±0.10	0.46 ±0.13	0.621 ±0.040	0.511 ±0.072	0.78 ±0.19
$pp \rightarrow \pi^- X$		1.22 ±0.13		2.74 ±0.16	1.322 ±0.074	0.489 ±0.038	0.249 ±0.024	0.078 ±0.013	0.017 ±0.006		1.34 ±0.12	0.236 ±0.032	0.011 ±0.008
$pC \rightarrow \pi^- X$		7.37 ±0.73	0.181 ±0.080	20.1 ±1.5	9.40 ±0.66	2.60 ±0.36	1.51 ±0.20	0.333 ±0.080	0.094 ±0.067	0.031 ±0.021	11.45 ±0.92	2.45 ±0.32	0.092 ±0.048
$pAl \rightarrow \pi^- X$				35.2 ±2.7		4.87 ±0.65	1.96 ±0.41	0.40 ±0.14	0.18 ±0.13	0.011 ±0.038			
$pCu \rightarrow \pi^- X$		19.0 ±2.0	0.24 ±0.22	51.0 ±4.3	24.8 ±1.7	9.1 ±1.1	4.07 ±0.63	0.94 ±0.25	0.29 ±0.14	0.114 ±0.085	30.4 ±2.6	5.30 ±0.76	0.154 ±0.080
$pAg \rightarrow \pi^- X$				77 ±10		4.83 ±0.96	1.55 ±0.55	0.42 ±0.25	0.08 ±0.14				
$pPb \rightarrow \pi^- X$		28.5 ±5.1	0.55 ±0.65	124.7 ±9.9	37.7 ±5.8	10.5 ±2.7	5.8 ±1.4	1.27 ±0.60	0.38 ±0.40	0.30 ±0.21	53.2 ±5.1	8.0 ±1.6	0.36 ±0.28
σ_0 (mb)		2.17 ±0.49	0.09 ±0.12	4.28 ±0.62	2.59 ±0.43	0.72 ±0.19	0.41 ±0.12	0.077 ±0.041	0.026 ±0.033	0.002 ±0.004	3.00 ±0.51	0.86 ±0.25	0.031 ±0.041
α		0.501 ±0.061	0.27 ±0.43	0.622 ±0.036	0.529 ±0.045	0.560 ±0.075	0.518 ±0.076	0.57 ±0.14	0.56 ±0.31	0.91 ±0.44	0.545 ±0.042	0.428 ±0.076	0.41 ±0.34
$pp \rightarrow K^+ X$				0.97 ±0.16	0.385 ±0.095	0.165 ±0.071	0.130 ±0.022	0.056 ±0.018	0.020 ±0.012		0.44 ±0.12	0.088 ±0.028	0.035 ±0.014

TABLE II. (*Continued.*)

P_t	p (GeV/c)	0.18 GeV/c				0.3 GeV/c				0.5 GeV/c			
		50	80	30	40	50	60	70	80	88	30	50	80
$pC \rightarrow K^+X$				5.28 ±0.98	3.39 ±0.35	1.65 ±0.29	1.36 ±0.29	0.59 ±0.12	0.160 ±0.063	0.085 ±0.028	3.23 ±0.73	1.21 ±0.35	0.158 ±0.095
$pAl \rightarrow K^+X$				8.7 ±1.3		2.64 ±0.55	2.31 ±0.55	0.96 ±0.36	0.75 ±0.32	0.121 ±0.050			
$pCu \rightarrow K^+X$				14.8 ±2.1	9.6 ±1.4	4.57 ±0.86	1.90 ±0.68	1.01 ±0.31	0.22 ±0.16	0.135 ±0.071	7.3 ±2.0	3.9 ±1.3	0.36 ±0.17
$pAg \rightarrow K^+X$				16.6 ±3.1		6.3 ±1.4	3.8 ±1.2	0.54 ±0.65	1.06 ±0.65	0.21 ±0.14			
$pPb \rightarrow K^+X$				37.3 ±5.6	21.5 ±3.3	8.1 ±2.0	4.3 ±1.7	1.4 ±1.2	1.01 ±0.49	0.33 ±0.39	20.7 ±5.7	7.8 ±3.2	0.43 ±0.43
σ_0 (mb)				1.04 ±0.34	0.68 ±0.16	0.40 ±0.14	0.56 ±0.27	0.33 ±0.20	0.039 ±0.035	0.034 ±0.030	0.65 ±0.34	0.23 ±0.15	0.063 ±0.081
α				0.638 ±0.079	0.645 ±0.062	0.580 ±0.090	0.37 ±0.13	0.24 ±0.18	0.56 ±0.24	0.36 ±0.26	0.62 ±0.13	0.67 ±0.16	0.40 ±0.33
$pp \rightarrow K^-X$		0.070 ±0.057		0.194 ±0.072	0.096 ±0.026	0.032 ±0.011	0.016 ±0.007						
$pC \rightarrow K^-X$		0.48 ±0.21		1.14 ±0.56	0.71 ±0.21	0.24 ±0.12	0.157 ±0.072				1.03 ±0.40	0.07 ±0.15	
$pAl \rightarrow K^-X$				2.6 ±1.2		0.17 ±0.17							
$pCu \rightarrow K^-X$		1.24 ±0.60		2.4 ±1.6	2.35 ±0.57	0.64 ±0.34	0.14 ±0.25				2.3 ±1.1	0.44 ±0.50	

TABLE II. (Continued.)

P_t	p (GeV/c)	0.18 GeV/c				0.3 GeV/c				0.5 GeV/c			
		50	80	30	40	50	60	70	80	88	30	50	80
$p\text{Ag} \rightarrow K^- X$				9.1 ±5.9			0.03 ±0.41	0.27 ±0.32					
$p\text{Pb} \rightarrow K^- X$	4.2 ±2.5		5.9 ±5.7	2.8 ±2.0	1.1 ±1.0	0.43 ±0.43	0.20 ±0.35				5.2 ±3.3	0.99 ±0.97	
σ_0 (mb)	0.079 ±0.086		0.30 ±0.31	0.18 ±0.12	0.039 ±0.055	0.11 ±0.16					0.26 ±0.25	0.01 ±0.03	
α	0.70 ±0.28		0.58 ±0.29	0.58 ±0.17	0.62 ±0.38	0.14 ±0.49					0.54 ±0.25	0.88 ±0.67	
$p\bar{p} \rightarrow pX$			5.68 ±0.29	6.47 ±0.33	8.59 ±0.40	10.10 ±0.20	10.82 ±0.21	11.87 ±0.18	13.74 ±0.28		2.93 ±0.18	3.82 ±0.12	4.173 ±0.066
$p\text{C} \rightarrow pX$			43.2 ±2.4	49.2 ±1.2	49.9 ±1.5	54.4 ±2.3	61.0 ±1.4	58.8 ±1.2	61.66 ±0.95		25.7 ±1.6	29.6 ±1.6	24.1 ±1.0
$p\text{Al} \rightarrow pX$			76.1 ±3.3		83.2 ±2.8	82.9 ±3.4	95.9 ±4.1	87.6 ±3.5	89.9 ±1.6				
$p\text{Cu} \rightarrow pX$			127.4 ±5.2	133.2 ±4.6	131.8 ±4.3	129.0 ±5.4	132.3 ±3.9	137.2 ±3.6	137.6 ±2.9		74.6 ±5.0	81.2 ±5.1	53.9 ±2.5
$p\text{Ag} \rightarrow pX$			176.0 ±8.3		175.5 ±6.5	179.2 ±8.5	193 ±11	178.6 ±6.4	171.5 ±4.7				
$p\text{Pb} \rightarrow pX$			242 ±13	248 ±11	228.2 ±9.6	225 ±11	249 ±17	247.7 ±7.9	217.7 ±6.8		138 ±11	115.1 ±9.6	89.4 ±5.4
σ_0 (mb)			10.11 ±0.93	11.89 ±0.67	13.28 ±0.77	15.5 ±1.2	18.2 ±1.1	16.71 ±0.77	19.94 ±0.69		5.94 ±0.80	8.8 ±1.0	7.66 ±0.71

TABLE II. (*Continued.*)

P_t	p (GeV/c)	0.18 GeV/c				0.3 GeV/c				0.5 GeV/c			
		50	80	30	40	50	60	70	80	88	30	50	80
α				0.605 ± 0.022	0.574 ± 0.016	0.546 ± 0.015	0.509 ± 0.020	0.487 ± 0.017	0.506 ± 0.012	0.457 ± 0.009	0.597 ± 0.034	0.501 ± 0.031	0.465 ± 0.024
$pp \rightarrow \bar{p}X$				0.090 ± 0.040	0.029 ± 0.013								
$pC \rightarrow \bar{p}X$	0.079 ± 0.098	0.000 ± 0.043		1.02 ± 0.35	0.12 ± 0.10	0.113 ± 0.086	0.018 ± 0.034	0.000 ± 0.016	0.000 ± 0.027	0.000 ± 0.012	0.10 ± 0.16	0.000 ± 0.025	
$pAl \rightarrow \bar{p}X$				0.87 ± 0.53			0.103 ± 0.094	0.000 ± 0.034	0.000 ± 0.059	0.000 ± 0.026			
$pCu \rightarrow \bar{p}X$	0.35 ± 0.30	0.00 ± 0.13		1.57 ± 0.86	0.48 ± 0.30	0.30 ± 0.34	0.04 ± 0.15	0.000 ± 0.048	0.000 ± 0.083	0.000 ± 0.036	1.87 ± 0.77	0.000 ± 0.077	
$pAg \rightarrow \bar{p}X$				1.4 ± 2.1				0.00 ± 0.21	0.000 ± 0.092				
$pPb \rightarrow \bar{p}X$	0.5 ± 1.8	0.00 ± 0.59		8.9 ± 3.1	0.3 ± 1.2	0.2 ± 1.2	0.49 ± 0.72		0.00 ± 0.37	0.00 ± 0.16	0.5 ± 3.6	0.00 ± 0.34	
σ_0 (mb)		0.012 ± 0.033		0.12 ± 0.12	0.029 ± 0.051	0.036 ± 0.081	0.002 ± 0.007						
α		0.79 ± 0.73		0.68 ± 0.25	0.62 ± 0.49	0.46 ± 0.71	0.95 ± 0.88						

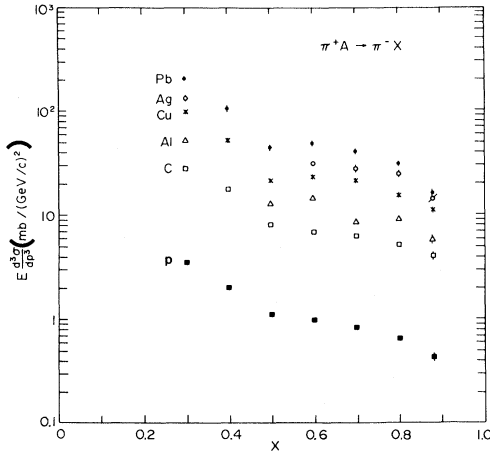


FIG. 3. The invariant differential cross section for $\pi^+A \rightarrow \pi^-X$ plotted as a function of x for an incident momentum of 100 GeV/c and transverse momentum of 0.3 GeV/c.

ciencies. The corrected rates were then used to obtain the invariant differential cross section for every channel.

In addition to the nuclear targets, data were taken on a hydrogen target at $P=40$ and 80 GeV/c for $P_t=0.3$ GeV/c. The invariant cross sections for the high-statistics $\pi^+p \rightarrow \pi^+X$ and $pp \rightarrow pX$ channels measured in this experiment agree on the average with those previously quoted¹ to $(4\pm 2)\%$ in absolute value. Throughout this paper the quoted hydrogen cross sections are the statistically more accurate ones measured earlier.

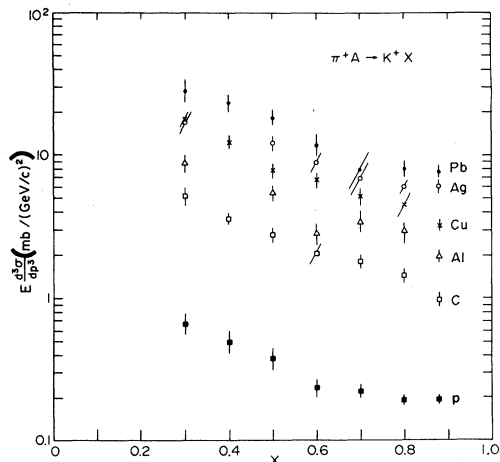


FIG. 4. The invariant differential cross section for $\pi^+A \rightarrow K^+X$ plotted as a function of x for an incident momentum of 100 GeV/c and transverse momentum of 0.3 GeV/c.

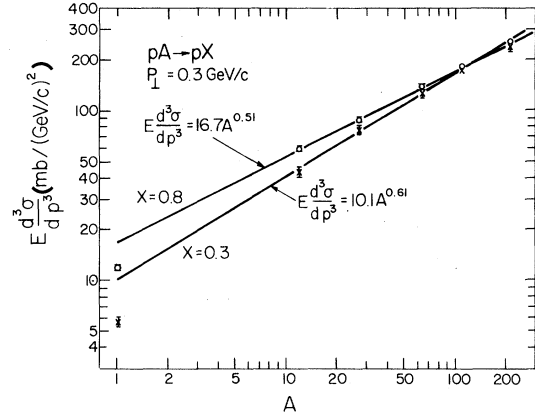


FIG. 5. The invariant differential cross section for $pA \rightarrow pX$ plotted as a function of A for $x=0.3$ and 0.8 at transverse momentum of 0.3 GeV/c. The straight lines are the best fits of the data to Eq. (1).

The complete set of measurements of the invariant cross sections is given in Table II. The errors are primarily statistical, but contain a small contribution from particle misidentification. The overall normalization uncertainty is estimated to be 10%. The only significant systematic uncertainties in the particle-misidentification corrections are those in the fractions of kaons called pions and nucleons. These systematic errors are estimated to be 5% and 0.4%, respectively. The corresponding systematic errors in the cross sections are everywhere less than the quoted statistical errors except for the reaction $K^+ \rightarrow \pi^+$ at $x=0.88$, where in any case the statistics are insufficient to determine a cross section.

As an illustration of the results, in Figs. 1–4 the invariant cross sections for $p \rightarrow p$, $p \rightarrow \pi^+$, $\pi^+ \rightarrow \pi^-$, and $\pi^+ \rightarrow K^+$ at $P_t=0.3$ GeV/c are plotted as a function of Feynman x .¹²

In order to exhibit explicitly the A dependence of the data, at every kinematic point the invariant cross sections were fitted to the empirical form

$$E \frac{d^3\sigma}{dp^3} = \sigma_0 A^\alpha. \quad (1)$$

Hydrogen data were not included in the fits. A typical data set and the fit to it are shown in Fig. 5. The results of all the fits are given in Table II. As can be seen from these results, as well as from most other nuclear target experiments, the extrapolation of Eq. (1) to $A=1$ does not yield the hydrogen result. This makes clear that conclusions drawn from experiments that use only one nuclear target in conjunction with hydrogen should be treated with caution.

III. DISCUSSION OF RESULTS

The A dependence of the inelastic cross sections on nuclei at 100 GeV can be parametrized as¹³ $25.8A^{0.76}$, $20.9A^{0.79}$, and $38.2A^{0.72}$ mb for incident π^+ , K^+ , and protons, respectively. The corresponding hydrogen cross sections are¹⁴ 20.2, 16.7, and 31.4 mb. A comparison of these values with those in Table II indicates that, over the entire projectile fragmentation region, and for all produced particles, the ratio of the inclusive cross section to the total inelastic cross section is smaller for a nuclear than for a proton target. Furthermore, this ratio decreases as the size of the nucleus increases.

As a test of the hypothesis of limiting fragmentation,² we can compare our incident-proton data at 100 GeV with those of Eichten *et al.*⁷ at 24 GeV. We find that the absolute values of the cross sections on nuclei are slightly higher at 24 GeV than at 100 GeV. A similar change is seen in proton target data over this energy range.¹⁵ The A dependences at the two energies are in very good agreement. We conclude that while the fragmentation of the projectile does depend on the nature of the target, the approach to scaling in Feynman x does not.

For the kinematic range covered by this experiment, the A dependence as expressed by the exponent α exhibits a remarkable simplicity. With a few exceptions, discussed later, it is only a function of x and incident particle type. It is independent of the outgoing particle type. To illustrate these

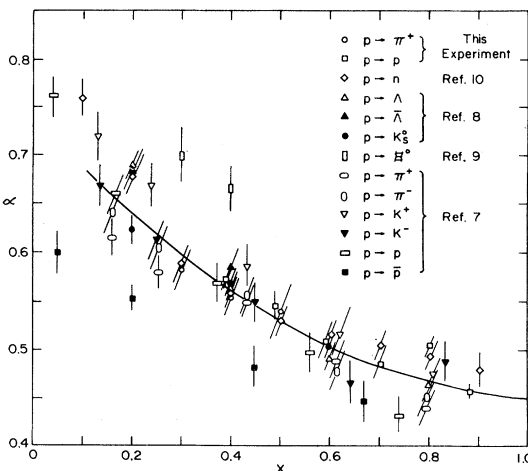


FIG. 6. The variation of the parameter α with x for various particles produced by protons at a transverse momentum of 0.3 GeV/c and for incident energies spanning the range 24–400 GeV. The curve is a polynomial fit to the data as discussed in the text. Closed symbols are used for all reaction channels where the incident and produced particle have no valence quarks in common.

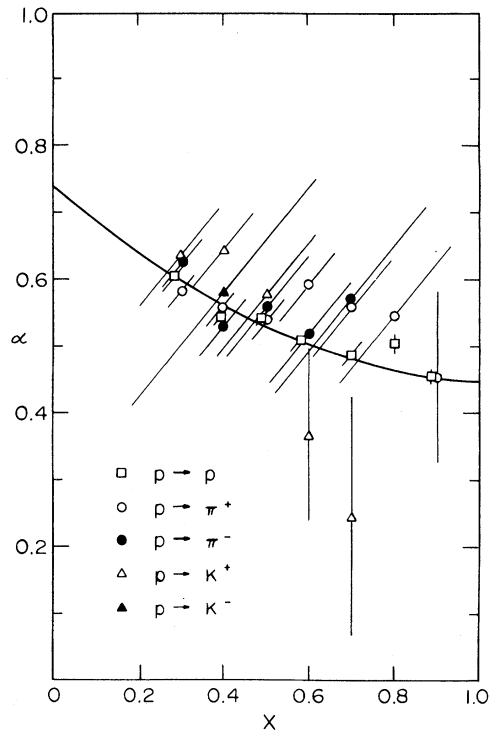


FIG. 7. The variation of the parameter α with x for our proton data at a transverse momentum of 0.3 GeV/c. The curve is the polynomial fit to the world data as discussed in the text. Error bars are shown slanted only for reasons of clarity.

features, in Fig. 6 we plot α as a function of x for a broad range of proton-induced reactions. In the interest of clarity, data points with errors in α greater than ± 0.03 have been omitted. The curve which has the functional form $\alpha(x) = 0.74 - 0.55x + 0.26x^2$ is a polynomial fit to all previous world data and data from this experiment. It has no particular significance other than to guide the eye. Although we have not plotted some statistically less significant results in Fig. 6, it should be pointed out that all our incident-proton data are well represented by the fitted curve, with $\chi^2/DF = 0.7$ (see Fig. 7). Except for $p \rightarrow \bar{p}$ at 24 GeV and $p \rightarrow \Xi^0$ at 400 GeV, the data in Fig. 6 for $x > 0.2$ suggest that α is a function of x alone. In other words, they suggest that, for a given x , the ratios of the production of various types of particles are independent of the target and of the incident energy.

If one takes this suggestion seriously and couples it to the observation that the functional form of $d\sigma/dx$ differs dramatically for various outgoing particles,¹ one seems to arrive at a very strong set of constraints on the possible mechanisms of particle production. For example, such behavior does not

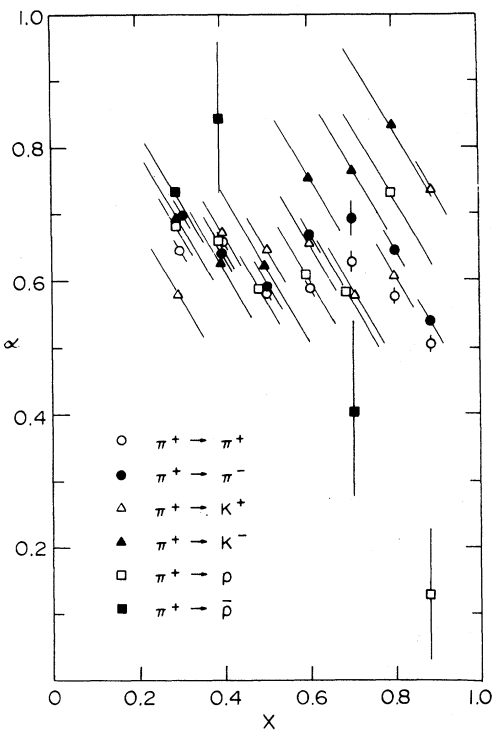


FIG. 8. The variation of the parameter α with x for the π^+ data at a transverse momentum of $0.3 \text{ GeV}/c$. Error bars are shown slanted only for reasons of clarity.

follow naturally from models such as the additive quark model,¹⁶ which assumes that the leading-particle spectrum is a reflection of the momentum spectrum of those valence quarks which are not absorbed in the target, nor does it follow from dual

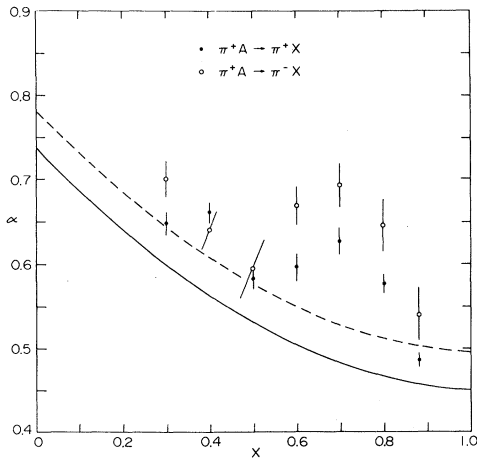


FIG. 9. The variation of the parameter α with x for the $\pi^+ \rightarrow \pi^+$ and $\pi^+ \rightarrow \pi^-$ channels at a transverse momentum of $0.3 \text{ GeV}/c$. The solid curve is the polynomial fit to the proton data shown in Fig. 6. The dashed curve is the same fit raised by 0.045 (see text).

parton models.¹⁷ This is most readily seen in the similarity of the A dependence of channels such as $p \rightarrow p$, $p \rightarrow \Lambda^0$, or $p \rightarrow \pi^+$ (open symbols in Fig. 6), where the projectile and outgoing particle have one or more valence quarks in common, to the A dependence of channels such as $p \rightarrow \bar{\Lambda}^0$, $p \rightarrow K_S^0$, or $p \rightarrow K^-$ (closed symbols), where there are no common valence quarks.

The data are also inconsistent with any mechanism whose essence is that the hadronic matter from the incident particle is slowed down as it passes through the target, and then decays into different particles in ratios independent of the final momentum of this hadronic matter. If this were the case, the ratios of particles at a given x on nuclear targets would be the same as the ratios from a proton target at a higher value of x , and not at the same x as is observed.

Finally, it is difficult to see how any multiple-collision model could account for the observed trends, in particular the constancy as a function of A of the ratios of the various produced particles at the highest values of x , i.e., greater than, say, 0.5. One possible mechanism which could explain such a constancy is that, at high x , particles are produced in collisions where only one target nucleon is involved. However, if this were so, α should be independent of x and should approach a value of about 0.31 for incident protons. This corresponds to the A dependence of the probability of a collision with a single nucleon in the nucleus.

A similar comprehensive study of π^+ - and K^+ -induced reactions is not possible because, as is apparent from Fig. 8, for most channels our statistical accuracy is inadequate, and no other comparable data exist. The only general conclusion that can be drawn from these data is that for π^+ - and K^+ -induced reactions, α tends to be higher than for proton-induced reactions. This may simply be a reflection of differences in the π , K , and p inelastic cross sections on nucleons.

Among the π and K data the only channels with

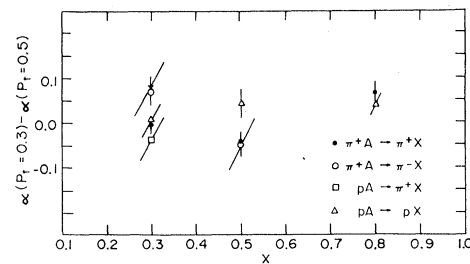


FIG. 10. The measured difference in the parameter α at transverse momentum 0.5 and $0.3 \text{ GeV}/c$ for various π^+ - and proton-induced reactions, as a function of x .

sufficient data to allow us to investigate the x dependences are $\pi^+ \rightarrow \pi^+$ and $\pi^+ \rightarrow \pi^-$. These results are replotted in Fig. 9, together with the polynomial fit to the proton data (solid curve) and the same fit displaced by 0.045, the difference in the A dependence of the inelastic cross section of pions and protons (dashed curve). These data suggest that the x dependence of α for π -induced reactions follows a universal curve similar to that observed in the proton data, but that superimposed on it for these particular channels there is an enhancement in α around an x value of 0.7. This enhancement can probably be explained entirely by the coherent production of the three- and five-pion states.¹⁸ At very low momentum transfers similar enhancements have been seen by Whalley *et al.*¹⁰ in the $p \rightarrow n$ channel.

In the past many experiments using emulsion targets have claimed that as x increases α first decreases and then increases towards a value equal to that of the inelastic cross section. This trend has been interpreted by some¹⁹ as an indication of a multiperipheral type of interaction. We see no evidence for such a trend.

Consistent with earlier experiments over the limited range in transverse momenta covered by our data, we find no significant variation of the A dependence as a function of P_t . In Fig. 10, for example, the difference of α at a P_t of 0.3 and 0.5 GeV/c is plotted as a function of x for $\pi^+ \rightarrow \pi^+$, $\pi^+ \rightarrow \pi^-$, $p \rightarrow \pi^+$, and $p \rightarrow p$. This behavior also excludes the interpretation of particle production in nuclei in terms of sequential collisions.

To summarize, we observe from our data and

from a comparison of our data with earlier experiments that the A dependence of the inclusive cross sections in the projectile fragmentation region exhibits a remarkable simplicity. For most channels the A dependence is a universal, weakly decreasing function of x independent of the outgoing particle, its transverse momentum, and the incident energy. The difference of the A dependences for various incident particles probably arises from the different inelastic cross sections on nucleons. We know of no model which in a natural way predicts such a simple behavior. However, it should be pointed out that most current models have sufficient flexibility to encompass the data. Our results do not rule out a weak dependence of α on the produced particle, and it is possible that α is not very sensitive to the mechanism of production. In the $\pi^+ \rightarrow \pi^\pm$ channels, there is evidence in our data for the presence of some coherent phenomena.

ACKNOWLEDGMENTS

We would like to express our thanks to the many people at the Fermi National Accelerator Laboratory who have contributed to the successful operation of this experiment, and to D. Dubin for assistance in data handling. Two of us (J.N. and T.S.) wish to thank Professor I.P. Zielinski for constant encouragement. This work was supported in part by the U.S. Department of Energy, the National Science Foundation Special Foreign Currency Program, and the Istituto Nazionale di Fisica Nucleare, Italy.

*Permanent address: Brookhaven National Laboratory, Upton, Long Island, New York 11973.

†Permanent address: High Energy Physics Laboratory, Harvard University, Cambridge, Massachusetts 02138.

‡Permanent address: Department of Physics, University of Illinois at Chicago Circle, Chicago, Illinois 60680.

§Present address: GTE, 77 A Street, Bldg. 5, Needham, Massachusetts 02194.

**Permanent address: Brookhaven National Laboratory, Upton, Long Island, New York 11973.

¹A. E. Brenner *et al.*, Phys. Rev. D **26**, 1497 (1982). A slight (<1%) change in absolute $hp \rightarrow h'p$ cross sections from this reference is due to a corrected treatment of the multiple interactions in the hydrogen target.

²J. Benecke *et al.*, Phys. Rev. **188**, 2159 (1969).

³See, for example, J. Elias *et al.*, Phys. Rev. D **22**, 13 (1980).

⁴See, for example, the reviews by N. N. Nikoleav, *Fiz. Elem. Chastits. At. Yadra* **12**, 162 (1981) [Sov. J. Part. Nucl. **12**, 63 (1981)]; W. Busza, in *Proceedings of the Hakone Seminar on High Energy Nuclear Interactions and Properties of Dense Nuclear Matter*, edited by K. Nakai and A. S. Goldhaber (Hayashi-Kobo Co. Ltd., Tokyo, 1980), Vol. II, p. 20.

⁵See, for example, A. Krzywicki *et al.*, Phys. Lett. **85B**, 407 (1979); G. Bertsch *et al.*, Phys. Rev. Lett. **47**, 297 (1981).

⁶A. S. Goldhaber, Nature (London) **275**, 114 (1978); W. Busza and A. S. Goldhaber, MIT Report No. MIT/LNS/CSC 82-2 (unpublished).

⁷T. Eichten *et al.*, Nucl. Phys. **B44**, 333 (1978).

⁸P. Skubic *et al.*, Phys. Rev. D **18**, 3115 (1978).

⁹L. Pondrom (private communication).

¹⁰M. R. Whalley *et al.*, University of Michigan Report No. UM HE 79-14, 1979 (unpublished).

¹¹P. H. Garbincius *et al.*, in *High Energy Physics—1980, proceedings of the XXth International Conference, Madison, Wisconsin*, edited by L. Durand and L. G. Pondrom (AIP, New York, 1981) p. 74; A. E. Brenner *et al.*, Report No. Fermilab-Conf-80/47-EXP 7160.451 (unpublished); D. S. Barton, in *Proceedings of the 11th International Symposium on Multiparticle Dynamics*,

- Bruges, Belgium, 1980*, edited by E. DeWolf and F. Verbeure (Univ. Antwerp, Antwerp, Belgium, 1980), p. 211; BNL Report No. 28166 (unpublished); C. Halliwell, *Acta Phys. Polon.* **B12**, 141 (1981).
- ¹²For all the targets x is defined as $P_{||}(\text{c.m.})/P_{||}(\text{max})$ (in cm) with the mass of the target taken to be the nucleon mass.
- ¹³A. S. Carroll *et al.*, *Phys. Lett.* **80B**, 319 (1979).
- ¹⁴See, for example, the compilation by G. Giacomelli, *Phys. Rep.* **23**, 123 (1976).
- ¹⁵See, for example, the compilation by F. E. Taylor *et al.*, *Phys. Rev. D* **14**, 1217 (1976).
- ¹⁶See, for example, V. V. Anisovich *et al.*, *Nucl. Phys.* **B133**, 477 (1978); N. N. Nikolaev and S. Pokorski, *Phys. Lett.* **80B**, 290 (1979); A. Dar and R. Takagi, *Phys. Rev. Lett.* **44**, 768 (1980); A. Bialas and W. Czyz, *Nucl. Phys.* **B194**, 21 (1982).
- ¹⁷A. Capella and J. Trần Thanh Vân, *Z. Phys. C* **10**, 249 (1981).
- ¹⁸A preliminary analysis of data on the coherent production of $\pi^+\pi^+\pi^-$ shows that most of the enhancement at $x=0.7$ is due to the decay of this particular coherently produced state [M. Zielinski (private communication)]. It should also be noted that in the $\pi^+p \rightarrow \pi^-X$ data the invariant cross section shows an enhancement in the same x region. For a possible interpretation of this phenomenon see the discussion in D. Cutts *et al.*, *Phys. Rev. Lett.* **40**, 141 (1978).
- ¹⁹See, for example, N. N. Nikolaev and L. D. Landau, ITP report, 1976 (unpublished).